

## 2-(6-Aryl-3(Z)-hexen-1,5-diynyl)anilines as a New Class of Potent Antitubulin Agents

Yu-Hsiang Lo,<sup>†,‡</sup> Ching-Chih Lin,<sup>‡,§</sup> Chi-Fong Lin,<sup>||</sup> Ying-Ting Lin,<sup>⊥</sup> Tsai-Hui Duh,<sup>∇</sup> Yi-Ren Hong,<sup>#</sup> Sheng-Huei Yang,<sup>∇</sup> Shinne-Ren Lin,<sup>∇</sup> Shyh-Chyun Yang,<sup>†</sup> Long-Sen Chang,<sup>Δ,X</sup> and Ming-Jung Wu<sup>\*,∇,X</sup>

Graduate Institute of Pharmaceutical Sciences, Graduate Institute of Biochemistry, Faculty of Biotechnology, Faculty of Medicinal and Applied Chemistry, Kaohsiung Medical University, Kaohsiung, Taiwan, Department of Biological Science and Technology, Chung Hwa College of Medical Technology, Tainan, Taiwan, Institute of Biomedical Science, National Sun Yat-Sen University, Kaohsiung, Taiwan, and National Sun Yat-Sen University-Kaohsiung Medical University Joint Research Center, Kaohsiung, Taiwan

Received July 9, 2007

Compounds **2a–h** and **6** displayed significant GI<sub>50</sub> values of 10<sup>-7</sup>–10<sup>-6</sup> M against various cancer cell lines. Of these compounds, 2-(6-(2-trifluoromethylphenyl))-3(Z)-hexen-1,5-diynylaniline (**2c**) showed the most potent growth inhibition activity. Compound **2c** also arrested cancer cells in the G2/M phase and in low concentration reduced a significant percentage of MDA-MB-231/ATCC breast cancer tetraploid cells. In addition to the G2/M block, compound **2c** caused microtubule depolymerization and induced apoptosis via activation of the caspase family.

### Introduction

Microtubules are cytoskeletal protein polymers formed by highly dynamic assemblies of tubulin heterodimers, including  $\alpha$ -tubulin and  $\beta$ -tubulin. Microtubules and their dynamics play a crucial role in many biological processes, including mitosis, intracellular transport, exocytosis, and cell growth.<sup>1a</sup> Since microtubules are important in mitosis and cell division, they have been a target for the development of a number of new anticancer drugs.<sup>1b</sup> There are two major groups of these antitumor agents: microtubule stabilizers such as paclitaxel<sup>2</sup> and microtubule destabilizers (colchicine,<sup>3</sup> combretastatin A-4,<sup>4</sup> and vinca alkaloids,<sup>5</sup> Chart 1) One of these compounds, combretastatin A-4 (CA-4), shows potent inhibition of microtubule polymerization by blocking colchicine's binding site and rapidly shutting down existing tumor vasculature.<sup>6</sup> Most of these compounds accumulate cells in the G2/M phase of cell cycle and induce apoptosis,<sup>7</sup> a cell suicide mechanism.

In our earlier publications<sup>8</sup> that described new enediyne antitumor agents, we found that 2-(6-(2-anilinyloxy)-3(Z)-hexen-1,5-diynyl)benzotrifluoride (**1**), which is structurally similar to CA-4, showed potent cytotoxic activity against all 60 tumor cell lines at a concentration of 10<sup>-7</sup> M. This compound is particularly potent against the MDA-MB-435 cell line of human breast cancer (0.11  $\mu$ M) and significantly arrested G2/M in the cell cycle and induced apoptosis. For further investigation of the role of G2/M phase blockage or to obtain lead compounds that would arrest the G2/M state more potently and with enhanced apoptotic effects, a series of 2-(6-aryl-3(Z)-hexen-1,5-diynyl)anilines **2a–h** and **6** were designed and synthesized. These

compounds were evaluated in the in vitro antitumor protocol of the NCI. They were also evaluated in the cell cycle analysis, the caspase-3 colorimetric assay, and microtubule depolymerization assay.

### Chemistry

The syntheses of the 2-(6-aryl-3(Z)-hexen-1,5-diynyl)anilines **2a–h** were carried out using vinyl chloride **3**<sup>9</sup> and 2-ethynylaniline **4**<sup>10</sup> as starting materials. The palladium-catalyzed Sonogashira coupling reaction<sup>11</sup> of **3** and **4** gave 2-(6-trimethylsilyl-3(Z)-hexen-1,5-diynyl)aniline (**5**) in 75% yield. Treatment of compound **5** with CuI in the presence of K<sub>2</sub>CO<sub>3</sub> in methanol gave **6** in 55% yield. Desilylation and palladium-catalyzed coupling reaction of **5** in the presence of K<sub>2</sub>CO<sub>3</sub> and MeOH with various aryl iodides (**7a–h**) gave **2a–h** in 34–78% yield. The results are summarized in Scheme 1.

### Biological Assay Results

**(A) Cytotoxicity Activities, Cell Cycle Analysis, and Caspase-3, -8, and -9 Activities.** Compounds **2a–h** and **6** were submitted to the National Cancer Institute for testing against a panel of approximately 60 tumor cell lines. Details of this test system have been published by others.<sup>12</sup> Compounds **2b** and **2d** are found to be inactive in the NCI screen, and the log<sub>10</sub> GI<sub>50</sub> values of the active compounds are shown in Table 1. The GI<sub>50</sub> values of these compounds are in the range 10<sup>-7</sup>–10<sup>-6</sup> M. Compound **2c** showed the most potent growth inhibitory activity against all tumor cell lines. In particular, compound **2c** displayed a two-digit nanomolar value of GI<sub>50</sub> against the SNB-75 of CNS cancer cell line. To investigate the mechanism of the inhibition activities of synthetic enediynes **2a–h** and **6**, we examined their cell cycle distribution by treating K-562 cells with these synthetic compounds for 24 h, and the cell cycle profile was analyzed by flow cytometry. The results are summarized in Table 2. Compounds **2c**, **2d**, and **2e** significantly blocked the K-562 cell cycle in the G2/M phase. The results indicated a significant increase of the G2/M phase percentage from 14.4% (control) to 73.9%, 81.4%, and 71.4% by compounds **2c**, **2d**, and **2e**, respectively. With the exception of potent G2/M cell cycle arrest, some of the enediyne derivatives also induced apoptosis in K-562 cells. Compared to the sub-G1 area (3.86%) of control, all compounds showed significant apoptotic

\* To whom correspondence should be addressed. Tel: 886-7-3121101 ext 2220. Fax: 886-7-3125339. E-mail: mijuwu@kmu.edu.tw.

<sup>†</sup> Graduate Institute of Pharmaceutical Sciences, Kaohsiung Medical University.

<sup>‡</sup> Contribution was equal to that of the first author.

<sup>§</sup> Department of Biological Sciences, National Sun Yat-Sen University.

<sup>||</sup> Department of Biological Science and Technology, Chung Hwa College of Medical Technology.

<sup>⊥</sup> Faculty of Biotechnology, Kaohsiung Medical University.

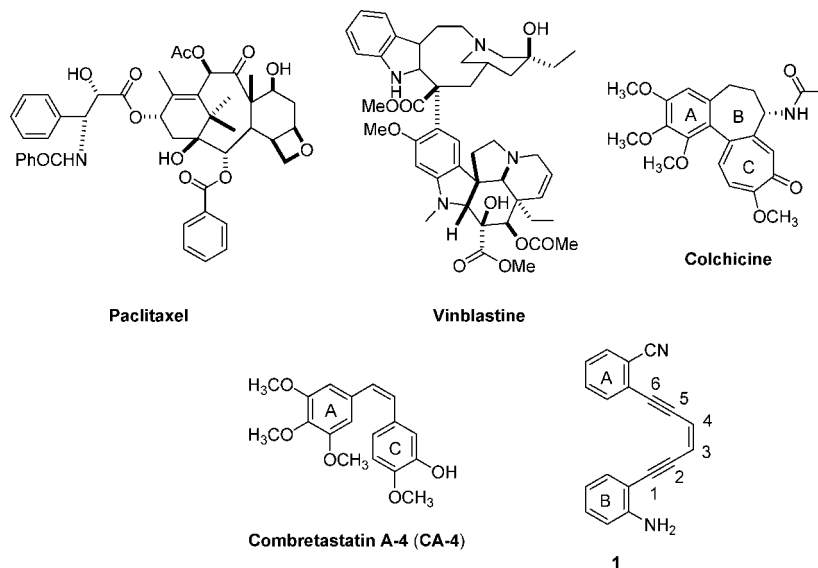
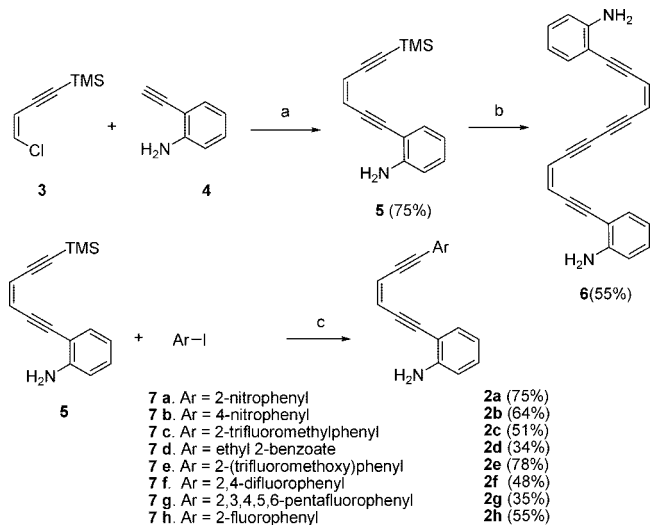
<sup>∇</sup> Faculty of Medicinal and Applied Chemistry, Kaohsiung Medical University.

<sup>#</sup> Graduate Institute of Biochemistry, Kaohsiung Medical University.

<sup>Δ</sup> Institute of Biomedical Science, National Sun Yat-Sen University.

<sup>X</sup> National Sun Yat-Sen University-Kaohsiung Medical University Joint Research Center.

## Chart 1

Scheme 1<sup>a</sup>

<sup>a</sup> Reagents and conditions: (a) Pd(PPh<sub>3</sub>)<sub>4</sub>, CuI, *n*BuNH<sub>2</sub>, ether, rt; (b) CuI, K<sub>2</sub>CO<sub>3</sub>, methanol, rt; (c) Pd(PPh<sub>3</sub>)<sub>4</sub>, CuI, K<sub>2</sub>CO<sub>3</sub>, methanol, rt.

activity (9.17% to 30.55%). More noteworthy is that compounds **2d** (28.68%), **2e** (30.55%), and **2g** (27.34%) have a greater ability to induce apoptosis.

Since compound **2c** is the most active compound among these synthetic enediynes, it was chosen to investigate the detailed mechanism of its action against the MDA-MB-231/ATCC breast cancer cell line. Parts A and B of Figure 1 display the cell cycle patterns of MDA-MB-231/ATCC treated with compound **2c** for 24 and 72 h, respectively. The concentration of **2c** chosen in this study is based on its LC<sub>50</sub> value against this tumor cell line (Supporting Information) and graduate diluted to 1/10th of that concentration. Thus, treatment of MDA-MB-231/ATCC cells with compound **2c** at different concentrations (3.6, 9.0, 18, 27, and 36 μM) for 24 h led to profound perturbations of the cell cycle profile with colchicine chosen as the control (Figure 1A). Our results show that cells treated with compound **2c** at a concentration of 3.6 μM for 24 h were sufficient to induce a massive accumulation of cells in the G<sub>2</sub>/M phase, and this phenomenon was also in a dose-dependent manner. In parallel to the G<sub>2</sub>/M block, a characteristic hypodiploid DNA content area (sub-G<sub>1</sub>) increased after 72 h of drug treatment at all doses

studied (Figure 1B). The detailed percentages are included in the Supporting Information. Moreover, the greatest accumulation of cells arrested in the G<sub>2</sub>/M stage occurred at 9 μM, and a relatively high concentration of **2c** (36 μM) led to the greatest apoptosis. However, all of these treatments were also correlated with the capacity to induce tetraploid (8N) cells (Figure 1A). The appearance of tetraploidy (8N) cells indicates that the cells went through an extra DNA replication without completing mitosis. Moreover, the phenomenon of generated tetraploidy can be induced by disrupting chromosome segregation during mitosis, disrupting the cell cleavage, or failed checkpoint control during mitosis.<sup>13</sup>

A major part of the phenomenon could be mediated by deregulation in cell cycle progression governed by families of caspases. Caspase-3, -8, and -9 in particular are the principal promoters of apoptosis. Colorimetric assays of caspase-3, -8, and -9 provided evidence of the relationship between compound **2c** and the programmed cell death. As shown in Figure 1C, apoptosis was shown by inducing caspase-3, -8, and -9 activities with 36 μM treatment for 72 h. It was demonstrated that the activity of caspase-3, -8, and -9 enhanced by 3.4, 4.0, and 3.9, respectively, relative to the control (Figure 1C). Taken together, our results suggested that the effects of compound **2c** on cell-cycle progression correlates well with its strong ability to induce a massive accumulation of cells in the G<sub>2</sub>/M phase and also to induce apoptosis via activation of caspase-3, -8, and -9.

**(B) Microtubule Depolymerization Assay.** The structure of synthetic enediyne **2c** is very similar to the skeleton of CA-4 or colchicines. For this reason, we anticipated that there is a relationship between the G<sub>2</sub>/M phase arrest caused by **2c** and microtubule function. To investigate the effect of **2c** upon microtubules, the microtubule depolymerization assay was carried out. Our data show that a brief exposure of the MDA-MB-231/ATCC cells to compound **2c** was sufficient to produce sustained depolymerization of the microtubules in a concentration-dependent manner (Figure 2). As shown in Figure 2, cells were treated with a low concentration (3.6 μM and 9 μM) of compound **2c** for 2 h. Microtubules were still seen in interphase cells, but their number was decreased and the microtubule cytoskeleton network was disorganized (Figure 2B,C), compared to the control cells (Figure 2A). At a higher concentration (18 and 27 μM), compound **2c** caused significant depolymerization

**Table 1.** In Vitro Screening of Eneidiynes, Colchicine, and CA-4 against the NCI's Cancer Cell Lines<sup>a</sup>

compd	log <sub>10</sub> GI <sub>50</sub> <sup>b</sup>						
	leukemia (K-562)	colon cancer (HCT-15)	CNS cancer (SNB-75)	melanoma (UACC-62)	ovarian cancer (OVCAR-3)	breast cancer (MDA-MB-231)	breast cancer (MDA-MB-435)
colchicine <sup>c</sup>	-7.9	-6.9	-7.6	-7.6	-7.8	-6.5	-8.0
combreastatin A-4 <sup>c</sup>	-7.5	-7.5	-6.1	-8.0	-7.4	-8.0	-7.5
<b>2a</b>	-6.3	-6.1	-4.9	-5.7	-5.4	-6.4	-6.4
<b>2c</b>	-6.0	-5.9	-7.1	-6.6	-6.2	-6.4	-6.4
<b>2e</b>	-5.6	-5.4	-5.6	-5.2	-5.4	-5.3	-5.9
<b>2f</b>	-5.3	-4.9	NA	-4.8	-5.2	-4.8	-5.6
<b>2g</b>	-4.8	-4.8	-4.4	-4.9	-4.8	-5.6	-4.8
<b>2h</b>	-5.5	-5.3	NA	-5.1	-5.5	-5.0	-5.7
<b>6</b>	-6.1	-5.4	-5.5	-5.7	-5.6	-5.8	-5.5

<sup>a</sup> Data obtained from the NCI's in vitro human tumor cell screen. NA = not available. <sup>b</sup> The concentration produces 50% reduction in cell growth. <sup>c</sup> The log<sub>10</sub>GI<sub>50</sub> of colchicine (NS C757) and combreastatin A-4(NSC613729) were obtained from NCI's web site (<http://dtp.nci.nih.gov/dtpstandard/dwindex/index.jsp>).

**Table 2.** Cell Cycle Distribution of K-562 Cell Line Treated with Synthetic Eneidiynes

cell cycle percentage <sup>a</sup>	<b>2a</b>	<b>2b</b>	<b>2c</b>	<b>2d</b>	<b>2e</b>	<b>2f</b>	<b>2g</b>	<b>2h</b>	<b>6</b>
G0/G1%	42.7	35.0	6.7	5.9	4.5	32.5	43.6	22.1	22.8
S%	41.0	46.2	19.3	12.7	24.1	33.1	38.5	40.9	25.0
G2/M%	16.3	18.8	73.9	81.4	71.4	34.4	17.9	37.0	52.2
Sub-G1 (apoptosis area)	11.13	15.78	19.40	28.68	30.55	10.04	27.34	9.19	11.52

<sup>a</sup> The percentages of the cells in each phase were calculated by using the WinMDI software for the flow cytometry treated with sample for 24 h used at a concentration of 50 μM by flow cytometry analysis. Control percentage: G0/G1 (26.7%), S (58.9%), G2/M (14.4%), and Sub-G1(3.86%).

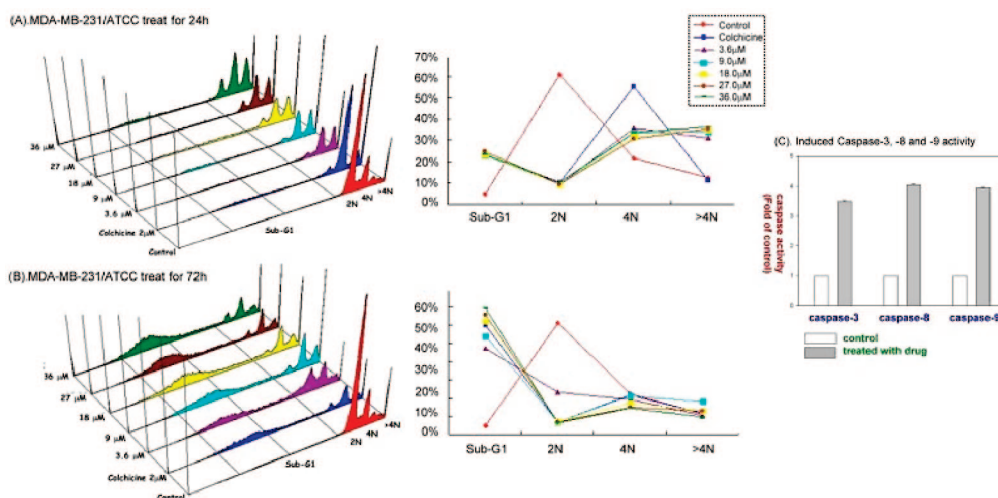


**Figure 1.** (A) Cell cycle distribution of MDA-MB-231/ATCC after treatment with compound **2c** at different concentrations for 24 h (A) and 72 h (B) and analyzed by flow cytometry G0/G1, S, and G2/M indicated the phase and sub-G1 area refers to the portion of apoptotic cells. (C) The caspase-3, -8, and -9 colorimetric assay of compound **2c** that absorption fold of control: caspase-3 (3.4), -8 (4.0), and -9(3.9), which can be quantified spectrophotometrically at a wavelength of 405 nm in 36 μM treatment for 72 h.

of microtubules in interphase cells (Figure 2D,E), and 36 μM compound **2c** induced extensive depolymerization of interphase microtubules (Figure 2F). In summary, these results suggest that the loss of function of microtubules in interphase cells treated with **2c** may prevent these cells from progressing into mitosis (Figures 1 and 2).

**(C) Microtubule Regrowth Assay.** To further examine whether the effect of compound **2c** on microtubule disassembly is reversible, the microtubule regrowth assay was carried out. MDA-MB-231/ATCC cells were treated with 36 μM of compound **2c** for 2 h, the drug was removed, and the cells were incubated in fresh culture medium for microtubule regrowth at the indicated time points as shown in Figure 3A–D. The well-known microtubule-depolymerizing agents, nocodazole and colchicine, were used as control. Nocodazole (Figure 3E–H) is a reversible antitubulin agent that was used as a positive control, and colchicine (Figure 3I–L) is an irreversible antitubulin agent that was employed as a negative control. As shown

in Figure 3, the disruption of microtubule assembly is reversible in a time-dependent manner when compound **2c** was removed (Figure 3A–D). Taken together, our data suggest that the effect of compound **2c** on microtubule depolymerization should be reversible.

**(D) Compound 2c Inhibits Tubulin Polymerization In Vitro.** To further explore whether the growth-inhibitory effect of these novel compounds was related to an interaction with the tubulin system, an in vitro tubulin polymerization assay was performed. The effects of **2c** (3.6, 9, 18, 27, and 36 μM) on microtubule formation were monitored by the increase in fluorescent intensity of the reaction mixture. As expected, colchicine (the positive control) potently inhibited tubulin polymerization and paclitaxel (the negative control) promoted the polymerization of tubulin. According to Figure 4, the IC<sub>50</sub> value of inhibition of tubulin polymerization for compound **2c** is about 9–10 μM and that for colchicine is much less than 3

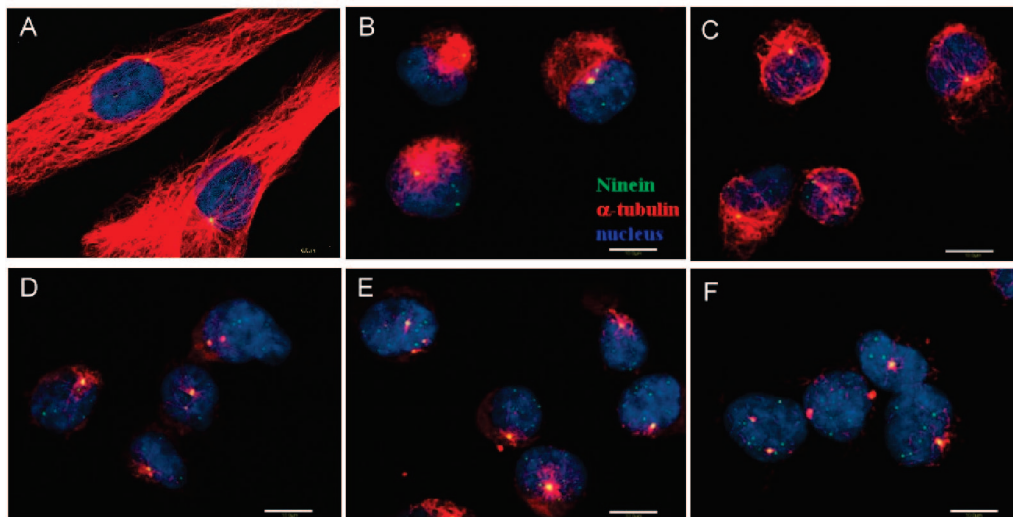


**Figure 2.** Dose effect of compound **2c** on microtubule depolymerization. MDA-MB-231/ATCC cells were treated with compound **2c** at 37 °C in 0 (A), 3.6 (B), 9 (C), 18 (D), 27 (E), and 36  $\mu\text{M}$  (F) for 2 h, respectively. Then cells were fixed and immunostained with antininein (green in merged images) antibody and anti- $\alpha$ -tubulin (red in merged images) antibody and counterstained with DAPI for nucleus staining. Scale bars represent 10  $\mu\text{M}$ .

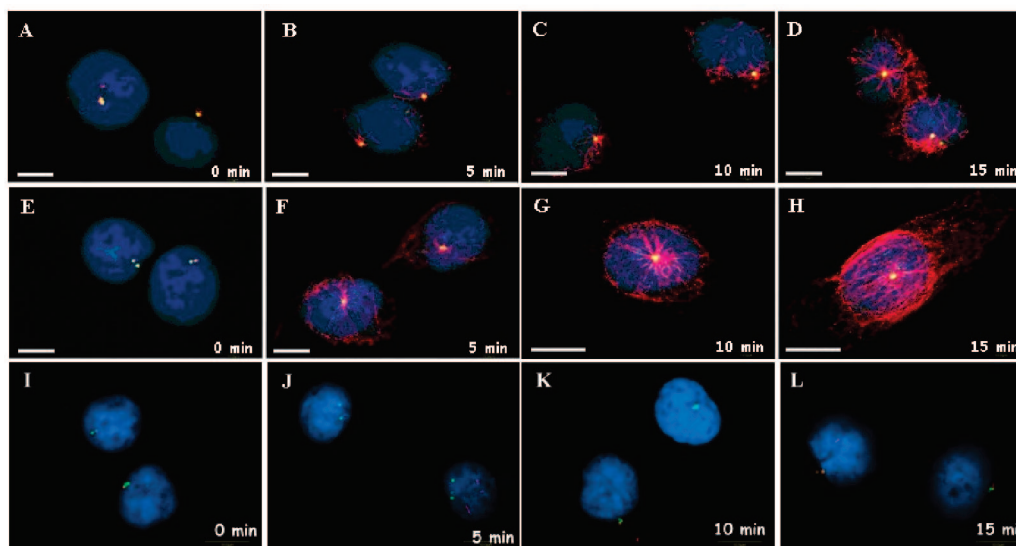


**Figure 3.** Effect of compound **2c** on depolymerization of microtubules is reversible. MDA-MB-231/ATCC cells were treated with compound **2c** in 36  $\mu\text{M}$  (A–D) and 20  $\mu\text{M}$  nocodazole (E, F) and 5  $\mu\text{M}$  colchicine (I–L) for 2 h at 37 °C. The drugs were then removed and the cells incubated in prewarmed medium at 37 °C for microtubule regrowth. Cells were fixed at the indicated time points and immunostained with antininein (green in merged images) antibody as a centrosome marker and anti- $\alpha$ -tubulin (red in merged images) antibody and counterstained with DAPI for nucleus staining. Scale bars represent 10  $\mu\text{M}$ .

$\mu\text{M}$ . Compound **2c** inhibited tubulin polymerization in a concentration-dependent manner (Figure 4).

### Conclusion

In this work, we have synthesized a series of 2-(6-aryl-3(Z)-hexen-1, 5-diynyl)anilines and found that these compounds show good growth inhibition activity against various human cancer cell lines. After a detailed investigation of the biological activities and mechanisms of activity of these synthetic enediynes, several conclusions can be reached: (i) The structure–activity relationship study shows that compound **2c** bearing a trifluoromethyl group at the 2-position on one of the phenyl rings, shows the most potent inhibitory activity. Introducing an oxygen atom into the trifluoromethylphenyl ring of **2c** to afford **2e** decreased the activity by 10-fold relative to the average  $\text{GI}_{50}$  values. When the trifluoromethyl group of **2c** was replaced

by fluoro atom as compound **2h**, the inhibition activity dropped dramatically. (ii) After a 24 h treatment with compound **2c**, a strong ability to induce a massive accumulation of cells in the G2/M phase was observed (Figure 1A). After 72 h treatment with compound **2c**, some of the cells undergo apoptosis via activation of caspase-3, -8, and -9 (Figure 1B,C). (iii) A brief exposure of the MDA-MB-231/ATCC cells to compound **2c** is sufficient to produce sustained depolymerization of the microtubules in a concentration-dependent manner (Figure 2). (iv) The disruption of microtubule is reversible when the drug is removed, which indicates a lower toxicity of this compound (Figure 3).

In conclusion, this study provides a new lead, such as compound **2**, for the development of antitumor agent and also provides a direction for further structure modification to obtain a more potent antitumor drug. We believe that the information

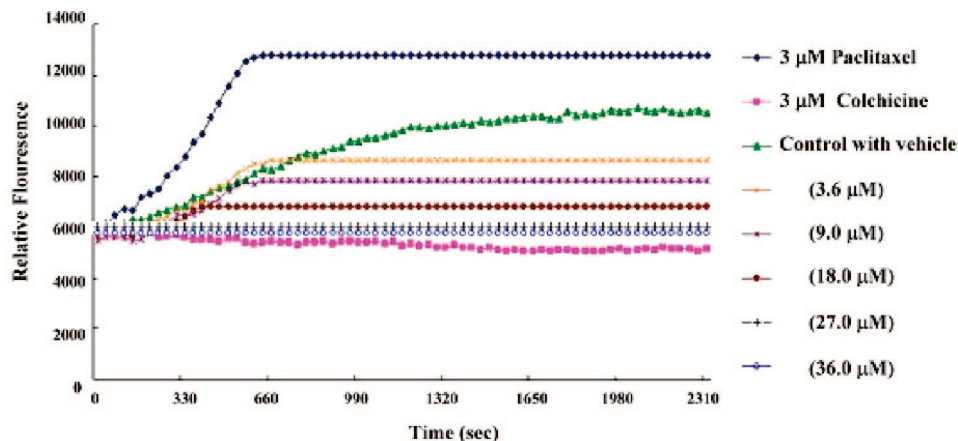


**Figure 4.** Pattern of various concentrations of compound **2c** on in vitro tubulin polymerization assay.

disclosed in this paper will have a significant impact upon the development of new anticancer drugs.

### Experimental Section

**Cell Culture.** (1) Human leukemia K-562 cells were obtained from the American Type Culture Collection (ATCC, Manassas, VA), and human purified lymphocyte preparation was obtained from blood as described previously. Cells were maintained in RPMI 1640 medium supplemented with 10% fetal calf serum, 2  $\mu$ M glutamine, and antibiotics (100 units/mL penicillin and 100  $\mu$ g/mL streptomycin) at 37  $^{\circ}$ C in a humidified atmosphere of 5% CO<sub>2</sub>.

(2) Human leukemia cells and MDA-MB-231/ATCC breast carcinoma cells were obtained from the American Type Culture Collection (ATCC, Manassas, VA), and human purified lymphocyte preparation was obtained from blood as described previously. K562 cells were maintained in RPMI 1640 medium supplemented with 10% fetal calf serum, 2  $\mu$ M glutamine, and antibiotics (100 units/mL penicillin and 100  $\mu$ g/mL streptomycin), and MDA-MB-231 cells were cultured in DMEM medium supplemented with 10% fetal bovine serum, 2  $\mu$ M glutamine, 1% nonessential amino acids, 100 units/mL penicillin, and 100  $\mu$ g/mL streptomycin (Gibco) at 37  $^{\circ}$ C in a humidified atmosphere of 5% CO<sub>2</sub>. Cell cultures were treated with compound **2c** (3.6, 9, 18, 27, or 36  $\mu$ M) and 20  $\mu$ M nocodazole (Sigma) in DMEM, respectively, at the indicated time periods before the cells were fixed.

**Cell Cycle Analysis.** Flow cytometry was used to measure cell cycle profile and apoptosis. For cell cycle analysis, K-562 cells treated with compounds **2a–h** and **6** (50  $\mu$ M) for 24 h were harvested by centrifugation. After being washed with PBS, the cells were fixed with ice-cold 70  $^{\circ}$ C ethanol for 30 min, washed with PBS, and then treated with 1 mL of 1 mg/mL of RNase A solution at 37  $^{\circ}$ C for 30 min. Cells were harvested by centrifugation at 1000 rpm for 5 min and further stained with 250  $\mu$ L of DNA staining solution (10 mg of propidium iodide [PI], 0.1 mg of trisodium citrate, and 0.03 mL of Triton X-100 were dissolved in 100 mL H<sub>2</sub>O) at room temperature for 30 min in the dark. After loading 500  $\mu$ L of PBS, the DNA contents of 10000 events were measured by FACSscan (Elite ESP, Beckman Coulter, Brea, CA) and the cell cycle profile was analyzed from the DNA content histograms with WinCycle software. When cells were apoptosis, those containing DNA were digested by endonuclease and then the sub G1 peak appeared. The percentage in sub G1 were analyzed by gating on cell cycle dot blots using Windows Multiple Document Interface software (WinMDI).

**Caspases Colorimetric Assay.** After different treatments, K-562 cells (1  $\times$  10<sup>6</sup> cells/mL) were collected and washed three times with PBS. Cells were resuspended in 200  $\mu$ L of cell lysis buffer (Biovision) and incubated on ice for 10 min. Cell lysates were clarified by centrifugation at 18000g for 3 min. The supernatant (cytosolic extract) was transferred to a fresh tube and kept on ice. The protein concentration in the supernatant was determined with

a BCA protein assay kit (Pierce, Rockford, IL), and clear lysates containing 50  $\mu$ g of protein were incubated with 100  $\mu$ M of enzyme-specific colorimetric substrates (Biovision) and 2 $\times$  reaction buffer (Biovision) containing 10 mM DTT at 37  $^{\circ}$ C for 1 h. The activity of caspases was described as the cleavage of colorimetric substrate by measuring the absorbance at 405 nm.<sup>14</sup>

**Immunocytochemistry and Microscopy.** These procedures were modified from previously described protocols.<sup>15</sup> In brief, MDA-MB-231/ATCC cells were grown on glass coverslips at a density of 1  $\times$  10<sup>4</sup> cells for 24 h. Cell cultures were rinsed several times with PBS, fixed in 4% paraformaldehyde for 5 min, and permeabilized with 0.5% Triton X-100 in PBS for 5 min. Fixed cells were rinsed in PBS, and nonspecific binding was blocked with 5% normal goat serum (NGS)/1% bovine serum albumin (BSA) in PBS pH 7.4 for at least 30 min at 37  $^{\circ}$ C. After a brief wash, the cells were incubated for 45 min at 37  $^{\circ}$ C with the primary antibodies diluted in the same blocking solution. After extensive washes with PBS, the cultures were then incubated with the appropriate secondary antibody conjugated to either Alexa 488 or Alexa 568 for 45 min at 37  $^{\circ}$ C. Finally, the cells were incubated for 5 min with DAPI (Roche) prior to mounting (Molecular Probes). Confocal images were obtained using an OLYMPUS IX71 microscope (100  $\times$  UPlanFI objective 1.3 NA) at 0.2  $\mu$ m z-steps, controlled by FLUOVIEW software (Universal Imaging). All images were imported into Adobe Photoshop v7.0 for contrast manipulation.

**Microtubule Regrowth Experiment.** MDA-MB-231/ATCC cells (1  $\times$  10<sup>4</sup>) were seeded on coverslips and grown for 24 h. Microtubules were depolymerized by treating with 3.6, 9, 18, 27, and 36  $\mu$ M **2c** in DMEM, respectively, for 2 h at 37  $^{\circ}$ C and 20  $\mu$ M nocodazole (Sigma) as control. For regrowth, cells were washed with PBS three times and incubated in prewarmed DMEM at 37  $^{\circ}$ C to allow regrowth. Cells were fixed at indicated time points and immunostained for ninein proteins and microtubules as described above.

**In Vitro Tubulin Polymerization Assay.** In vitro tubulin polymerization assays were conducted with reagents as described by the manufacturer (Cytoskeleton, Inc.). In brief, compound **2c** was incubated with purified bovine tubulin and buffer containing 20% glycerol and 1 mM GTP at 37  $^{\circ}$ C, and the effect of compound **2c** on tubulin polymerization was monitored kinetically using a fluorescent plate reader (FLUOstar galaxy, BMG).<sup>16</sup>

**2-(6-Trimethylsilyl-3(Z)-hexen-1,5-diynyl)aniline (5).** To a degassed solution of **4** (12 mmol) containing CuI (3.2 mmol) and *n*-BuNH<sub>2</sub> (30 mmol) in ether (20 mL) was added a degassed solution of compound **3** (12 mmol) containing Pd(PPh<sub>3</sub>)<sub>4</sub> (0.8 mmol) in ether (25 mL). The resulting reaction mixture was stirred at room temperature for 4 h and then quenched with saturated aqueous NH<sub>4</sub>Cl solution. The aqueous layer was extracted with EtOAc (30 mL  $\times$  3), and the combined organic extracts were washed with saturated aqueous Na<sub>2</sub>CO<sub>3</sub> solution (40 mL) and dried over anhydrous MgSO<sub>4</sub>. After filtration and removal of solvent in vacuo,

the residue was purified by column chromatography on silica gel (hexane/EA = 10:1 as the eluent) to give **5** in 75% yield as brown oil:  $^1\text{H NMR}$  ( $\text{CDCl}_3$ , 200 MHz)  $\delta$  7.33–7.28 (m, 1H), 7.15 (ddd, 1H,  $J = 8.2, 7.2, 1.6$  Hz), 6.73–6.65 (m, 2H), 6.13 (d, 1H,  $J = 11.0$  Hz), 5.88 (d, 1H,  $J = 11.0$  Hz), 4.32 (bs, 2H), 0.25 (s, 9H);  $^{13}\text{C NMR}$  ( $\text{CDCl}_3$ , 50 MHz)  $\delta$  148.1, 132.1, 130.3, 120.5, 117.8, 117.7, 114.1, 107.2, 102.9, 102.8, 94.4, 92.8, 0.0; HRMS calcd for  $\text{C}_{15}\text{H}_{17}\text{NSi}$ ,  $M_r = 239.1131$ , found 239.1127.

**6,6-Bis(3(Z)-hexen-1,5-diynyl)aniline (6)**. To a degassed solution of 2-(6-trimethylsilyl-3(Z)-hexen-1,5-diynyl)aniline (**5**) (0.1 g, 0.42 mmol) containing  $\text{K}_2\text{CO}_3$  (0.56 g, 4.2 mmol) in MeOH (20 mL) was added CuI (80 mg, 0.42 mmol). The resulting reaction mixture was stirred at room temperature for 3 h. Solvent was then removed in vacuo. The residue was quenched with saturated aqueous  $\text{NH}_4\text{Cl}$  solution and extracted with EtOAc (20 mL  $\times$  3). The combined organic extracts were washed with saturated aqueous  $\text{Na}_2\text{CO}_3$  solution (40 mL) and dried over anhydrous  $\text{MgSO}_4$ . After filtration and removal of solvent in vacuo, the residue was purified by column chromatography using hexane/EA (1:1) as eluent on silica gel to give the desired product **6** (76 mg, 55%) as a brown oil:  $^1\text{H NMR}$  ( $\text{CDCl}_3$ , 200 MHz)  $\delta$  7.28 (dd, 1H,  $J = 7.8, 1.2$  Hz), 7.04 (td, 1H,  $J = 7.4, 1.6$  Hz), 6.62 (td, 1H,  $J = 7.6, 1.2$  Hz), 6.46 (d, 1H,  $J = 8.8$  Hz), 6.31 (d, 1H,  $J = 10.2$  Hz), 5.96 (d, 1H,  $J = 10.6$  Hz), 4.44 (bs, 2H);  $^{13}\text{C NMR}$  ( $\text{CDCl}_3$ , 50 MHz)  $\delta$  148.5, 131.9, 130.6, 123.6, 117.5, 116.0, 114.3, 106.4, 96.6, 93.1, 83.1, 80.7; HRMS calcd for  $\text{C}_{24}\text{H}_{16}\text{N}_2$ ,  $M_r = 332.1313$ , found 332.1322.

**General Procedure for the Synthesis of Compounds 2a–h**. To a degassed solution of 2-(6-trimethylsilyl-3(Z)-hexen-1,5-diynyl)aniline (**5**) (12 mmol) containing CuI (3.2 mmol) and  $\text{K}_2\text{CO}_3$  (30 mmol) in MeOH (15 mL) was added a degassed solution of aryl iodides (**7a–h**) (12 mmol) containing  $\text{Pd}(\text{PPh}_3)_4$  (0.8 mmol) in MeOH (20 mL). The resulting reaction mixture was stirred at room temperature for 6 h. Solvent was then removed in vacuo. The residue was quenched with saturated aqueous  $\text{NH}_4\text{Cl}$  solution and extracted with EtOAc (20  $\times$  3 mL). The combined organic extracts were washed with saturated aqueous  $\text{Na}_2\text{CO}_3$  solution (40 mL) and dried over anhydrous  $\text{MgSO}_4$ . After filtration and removal of solvent in vacuo, the residue was purified by column chromatography on silica gel to give the desired products.

**2-(6-(2-Nitrophenyl)-3(Z)-hexen-1,5-diynyl)aniline (2a)**. This compound was obtained in 75% yield as a brown oil using hexane/EA (3:1) as eluent by the general procedure:  $^1\text{H NMR}$  ( $\text{CDCl}_3$ , 200 MHz)  $\delta$  8.06 (d, 1H,  $J = 8.0$  Hz), 7.70–7.38 (m, 3H), 7.11 (td, 2H,  $J = 4.8, 1.8$  Hz), 6.73–6.66 (m, 2H), 6.25 (dd, 2H,  $J = 11, 2.6$  Hz), 4.16 (bs, 2H);  $^{13}\text{C NMR}$  ( $\text{CDCl}_3$ , 50 MHz)  $\delta$  148.2, 135.1, 132.7, 132.2, 130.3, 128.7, 124.5, 121.3, 118.3, 117.6, 116.9, 114.1, 107.0, 95.5, 94.8, 92.6, 91.8; HRMS calcd for  $\text{C}_{18}\text{H}_{12}\text{N}_2\text{O}_2$ ,  $M_r = 288.0899$ , found 288.0890.

**2-(6-(4-Nitrophenyl)-3(Z)-hexen-1,5-diynyl)aniline(2b)**. This compound was obtained in 64% yield as a brown oil using hexane/EA (3:1) as eluent by the general procedure:  $^1\text{H NMR}$  ( $\text{CDCl}_3$ , 200 MHz)  $\delta$  8.20 (d, 2H,  $J = 8.2$  Hz), 7.63 (d, 3H,  $J = 8.8$  Hz), 7.41–7.20 (m, 3H), 6.88–6.67 (m, 2H), 6.28 (d, 1H,  $J = 10.6$  Hz), 6.09 (d, 1H,  $J = 11$  Hz), 4.11 (bs, 2H);  $^{13}\text{C NMR}$  ( $\text{CDCl}_3$ , 50 MHz)  $\delta$  148.1, 132.4, 132.0, 130.5, 123.8, 123.5, 121.7, 121.2, 117.9, 116.8, 114.2, 110.8, 102.6, 95.7, 94.6, 92.7, 92.6; HRMS calcd for  $\text{C}_{18}\text{H}_{12}\text{N}_2\text{O}_2$ ,  $M_r = 288.0899$ , found 288.0876.

**2-(6-(2-Trifluoromethylphenyl)-3(Z)-hexen-1,5-diynyl)aniline (2c)**. This compound was obtained in 51% yield as a brown oil using hexane/EA (3:1) as eluent by the general procedure:  $^1\text{H NMR}$  ( $\text{CDCl}_3$ , 200 MHz)  $\delta$  7.65 (t, 2H,  $J = 5.4$  Hz), 7.55–7.25 (m, 3H), 7.14 (td, 1H,  $J = 7.6, 1.4$  Hz), 6.69 (d, 2H,  $J = 4.8$  Hz), 6.25 (d, 1H,  $J = 1.4$  Hz), 6.20 (d, 1H,  $J = 1.8$  Hz), 4.8–4.2 (bs, 2H);  $^{13}\text{C NMR}$  ( $\text{CDCl}_3$ , 50 MHz)  $\delta$  147.0, 134.4, 132.1, 131.2, 130.3, 128.3, 127.3, 126.0, 125.9, 125.8, 120.5, 118.5, 117.6, 114.8, 108.0, 94.6, 92.9, 92.5; HRMS calcd for  $\text{C}_{19}\text{H}_{12}\text{F}_3\text{N}$ ,  $M_r = 311.0922$ , found 311.0896.

**2-(6-(2-Ethoxycarbonylphenyl)-3(Z)-hexen-1,5-diynyl)aniline (2d)**. This compound was obtained in 34% yield as a brown oil using hexane/EA (4:1) as eluent by the general procedure:  $^1\text{H NMR}$  ( $\text{CDCl}_3$ , 200 MHz)  $\delta$  7.89 (dd, 1H,  $J = 7.4, 2.4$  Hz), 7.66 (dd, 1H,

$J = 10.2, 3.6$  Hz), 7.52–7.21 (m, 4H), 7.11 (td, 1H,  $J = 7.4, 2.8$  Hz), 6.22 (d, 2H,  $J = 4.4$  Hz), 4.38 (q, 2H,  $J = 4.4$  Hz), 4.08 (bs, 1H), 1.40 (t, 3H,  $J = 3.4$  Hz);  $^{13}\text{C NMR}$  ( $\text{CDCl}_3$ , 50 MHz)  $\delta$  166.0, 148.2, 134.4, 132.1, 131.9, 131.4, 130.3, 130.1, 128.1, 123.1, 119.8, 118.0, 117.5, 114.0, 107.2, 95.6, 94.5, 93.0, 92.3, 61.2, 64.1; HRMS calcd for  $\text{C}_{21}\text{H}_{17}\text{NO}_2$ ,  $M_r = 315.1259$ , found 315.1253.

**2-(6-(2-(Trifluoromethoxy)phenyl)-3(Z)-hexen-1,5-diynyl)aniline (2e)**. This compound was obtained in 78% yield as a brown oil using hexane/EA (4:1) as eluent by the general procedure:  $^1\text{H NMR}$  ( $\text{CDCl}_3$ , 400 MHz)  $\delta$  7.56 (dd, 1H,  $J = 8.0, 1.6$  Hz), 7.38–7.27 (m, 3H), 7.14 (td, 1H,  $J = 7.6, 1.2$  Hz), 6.72–6.68 (m, 2H), 6.22 (d, 1H,  $J = 10.8$  Hz), 6.11 (d, 1H,  $J = 10.8$  Hz) 4.20 (bs, 2H);  $^{13}\text{C NMR}$  ( $\text{CDCl}_3$ , 100 MHz)  $\delta$  147.8, 134.8, 134.7, 134.1, 132.1, 130.3, 127.8, 127.7, 121.1, 120.4, 118.0, 117.5, 114.4, 94.7, 92.9, 92.5, 90.8; HRMS calcd for  $\text{C}_{19}\text{H}_{12}\text{F}_3\text{NO}$ ,  $M_r = 327.0871$ , found 327.0877.

**2-(6-(2,4-Difluorophenyl)-3(Z)-hexen-1,5-diynyl)aniline (2f)**. This compound was obtained in 48% yield as a yellow oil using hexane/EA (3:1) as eluent by the general procedure:  $^1\text{H NMR}$  ( $\text{CDCl}_3$ , 400 MHz)  $\delta$  7.50–7.44 (m, 1H), 7.32 (dd, 1H,  $J = 7.6, 1.2$  Hz), 7.15 (td, 1H,  $J = 6.8, 1.6$  Hz), 6.91–6.85 (m, 2H), 6.73–6.69 (m, 2H), 6.20 (d, 1H,  $J = 10.8$  Hz), 6.07 (d, 1H,  $J = 11.2$  Hz), 4.00 (bs, 2H);  $^{13}\text{C NMR}$  ( $\text{CDCl}_3$ , 100 MHz)  $\delta$  134.7, 134.6, 132.1, 130.4, 120.2, 117.9, 117.3, 114.4, 111.8, 111.6, 107.4, 104.6, 104.3, 104.1, 94.8, 92.9, 92.3, 89.1; HRMS calcd for  $\text{C}_{18}\text{H}_{11}\text{F}_2\text{N}$ ,  $M_r = 279.0860$ , found 279.0866.

**2-(6-(2,3,4,5,6-Pentafluorophenyl)-3(Z)-hexen-1,5-diynyl)aniline (2g)**. This compound was obtained in 35% yield as a yellow oil using hexane/EA (3:1) as eluent by the general procedure:  $^1\text{H NMR}$  ( $\text{CDCl}_3$ , 400 MHz)  $\delta$  7.31–7.26 (m, 1H), 7.04 (t, 1H,  $J = 7.2, 1.2$  Hz), 6.73–6.60 (m, 2H), 6.29 (d, 1H,  $J = 5.2$  Hz), 5.97 (d, 1H,  $J = 10.4$  Hz), 4.12 (bs, 2H);  $^{13}\text{C NMR}$  ( $\text{CDCl}_3$ , 100 MHz)  $\delta$  148.5, 132.1, 130.6, 130.5, 123.8, 123.7, 118.0, 117.7, 117.5, 116.2, 116.0, 114.3, 114.2, 106.8, 96.6, 94.1, 83.1, 82.4; HRMS calcd for  $\text{C}_{18}\text{H}_8\text{F}_5\text{N}$ ,  $M_r = 333.0577$ , found 333.0580.

**2-(6-(2-Fluorophenyl)-3(Z)-hexen-1,5-diynyl)aniline (2h)**. This compound was obtained in 55% yield as a yellow oil using hexane/EA (3:1) as eluent by the general procedure:  $^1\text{H NMR}$  ( $\text{CDCl}_3$ , 200 MHz)  $\delta$  7.49 (td, 1H,  $J = 9.8, 1.6$  Hz), 7.39–7.28 (m, 2H), 7.18–7.05 (m, 3H), 6.73–6.65 (m, 2H), 6.21 (d, 1H,  $J = 10.8$  Hz), 6.10 (d, 1H,  $J = 10.8$  Hz), 4.41 (bs, 2H);  $^{13}\text{C NMR}$  ( $\text{CDCl}_3$ , 50 MHz)  $\delta$  148.3, 133.8, 132.1, 130.5, 130.3, 124.1, 124.0, 120.1, 117.6, 117.4, 115.7, 115.3, 114.1, 107.2, 94.9, 92.9, 92.5, 90.1; HRMS calcd for  $\text{C}_{18}\text{H}_{12}\text{FN}$ ,  $M_r = 261.0954$ , found 261.0949.

**Acknowledgment.** We thank the National Science Council of the Republic of China and National Sun Yat-Sen University-Kaohsiung Medical University Joint Research Center for financial support and the National Institutes of Health (National Cancer Institute) for the cytotoxicity screening.

**Supporting Information Available:** Data for the cell cycle percentage for 24 and 72 h, HPLC purity data, and full panel screening data of **2c**. This material is available free of charge via the Internet at <http://pubs.acs.org>.

## References

- (1) (a) Jordan, M. A.; Wilson, L. Microtubule and Actin filaments: dynamic targets for cancer chemotherapy. *Curr. Opin. Cell Biol.* **1998**, *10*, 123–130. (b) Jordan, M. A.; Wilson, L. Microtubules as a Target for Anticancer Drugs. *Nature Rev. Cancer* **2004**, *4*, 253–265.
- (2) Schiff, P. B.; Fant, J.; Horwitz, S. B. Promotion of microtubule assembly *in vitro* by Taxol. *Nature* **1979**, *277*, 665–667.
- (3) Li, Q.; Sham, H.; Rosenberg, S. Antimitotic agents. *Annu. Rep. Med. Chem.* **1999**, *34*, 139–148.
- (4) Nam, N. H. Combretastatin A-4 Analogues as Antimitotic Antitumor Agents. *Cur. Med. Chem.* **2003**, *10*, 1697–1722.
- (5) Jordan, M. A.; Hadfield, J. A.; Lawrence, N. J.; McGown, A. T. Tubulin as a target for anticancer drugs: agents which interact with the mitotic spindle. *Med. Res. Rev.* **1998**, *18*, 259–296.
- (6) (a) Tozer, G. M.; Kanthou, C.; Parkins, C. S.; Hill, S. A. The Biology of the Combretastatins as Tumour Vascular Targeting Agents. *Int. J. Exp. Pathol.* **2002**, *83*, 21–38. (b) Prise, V. E.; Honess,

- D. J.; Stratford, M. R.; Wilson, J.; Tozer, G. M. The Vascular Response of Tumor and Normal Tissues in the Rat to the Vascular Targeting Agent. Combretastatin A-4-Phosphate at Clinically Relevant Doses. *Int. J. Oncol.* **2003**, *21*, 717–726.
- (7) Vitale, I.; Antocchia, A.; Cenciarelli, C.; Crateri, P.; Meschini, S.; Arancia, G.; Pisano, C.; Tanzarella, C. Combretastatin (CA-4) and combretastatin derivative induce mitotic catastrophe dependent on spindle checkpoint and caspase-3 activation in non-small cell lung cancer cells. *Apoptosis* **2006**, *12*, 155–166.
- (8) (a) Lo, Y. H.; Lin, C. F.; Hsieh, M. C.; Wu, M. J. Remarkable G2/M phase arrest and apoptotic effect performed by 2-(6-aryl-3-hexen-1,5-diynyl) benzonitrile antitumor agents. *Bioorg. Med. Chem.* **2004**, *12*, 1047–1053. (b) Lin, C. F.; Lo, Y. H.; Hsieh, M. C.; Chen, Y. H.; Wang, J. J.; Wu, M. J. Cytotoxicities, cell cycle and caspase evaluations of 1,6-diaryl-3(Z)-hexen-1,5-diynes, 2-(6-aryl-3(Z)-hexen-1,5-diynyl)anilines and their derivatives. *Bioorg. Med. Chem.* **2005**, *13*, 3565–3575.
- (9) Alami, M.; Gueugnot, S.; Domingues, E.; Linstrumelle, G. An efficient synthesis of 1,3(E), 5(Z), 1,3(E), 5(E) and 1,3(Z), 5(Z)-trienes: Application to the synthesis of galbanolenes and (9Z,11E)-9,11,13-tetradecatrien-1-yl acetate. *Tetrahedron* **1995**, *51*, 1209–1220.
- (10) Koradin, C.; Dohle, W.; Alain, L.; Rodriguez, A. L.; Schmid, B.; Knochel, P. Synthesis of polyfunctional indoles and related heterocycles mediated by cesium and potassium bases. *Tetrahedron* **2003**, *59*, 1571–1587.
- (11) Negishi, E. I.; Anastasia, L. Palladium-Catalyzed Alkynylation. *Chem. Rev.* **2003**, *103*, 1979–2107.
- (12) Boyd, M. R.; Paull, K. D. Some practical considerations and applications of the National Cancer Institute in vitro anticancer drug discovery screen. *Drug Dev. Res.* **1995**, *34*, 91–104.
- (13) Robert, L.; Margolis, R. L.; Lohez, O. D.; Andreassen, P. R. G1 Tetraploidy Checkpoint and the Suppression of Tumorigenesis. *J. Cell. Biochem.* **2003**, *88*, 673–683.
- (14) Wu, Z. Z.; Chien, C. M.; Yang, S. H.; Lin, Y. H.; Hu, X. W.; Lu, Y. J.; Wu, M. J.; Lin, S. R. Induction of G2/M phase arrest and apoptosis by a novel enediyne derivative, THDA, in chronic myeloid leukemia (K562) cells. *Mol. Cell. Biol.* **2006**, *292*, 99–105.
- (15) Lin, C. C.; Cheng, T. S.; Hsu, C. M.; Wu, C. H.; Chang, L. S.; Shen, Z. S.; Yeh, H. M.; Chang, L. K.; Howng, S. L.; Hong, Y. R. Characterization and functional aspects of human ninein isoforms that regulated by centrosomal targeting signals and evidence for docking sites to direct gamma-tubulin. *Cell Cycle* **2006**, *5*, 2517–2527.
- (16) Duan, J. X.; Cai, X.; Meng, F.; Lan, L.; Hart, C.; Matteucci, M. Potent Antitubulin Tumor Cell Cytotoxins Based on 3-Aroyl Indazoles. *J. Med. Chem.* **2007**, *50*, 1001.

JM070820N